Defence Science Journal, Vol 46, No. 4, October 1996, pp. 223-232

Simulated & Experimental In-Wall Temperatures for 120 mm Ammunition

M.L. Bundy and P.J. Conroy
US Army Research Laboratory, Aberdeen Proving Ground, MD 21005-5066

and

J. L. Kennedy
Alliant Techsystems, Inc., Hopkins, MN

ABSTRACT

Bore and chamber surface, as well as subsurface, temperature predictions are made for the US Army M256 120 mm chromium-plated cannon firing M865, M829, and DM13 cartridges. The surface temperature predictions are validated by comparison with other numerical modelling results, while the subsurface temperature predictions are compared directly with experimental measurements made by in-wall thermocouples. The surface temperature predictions fall in line with other numerical estimates, and, in general, the simulated probe temperatures at each axial location are within the circumferential and round-to-round variation in the experimental probe temperatures.

1. INTRODUCTION

Bore erosion models require accurate predictions of surface and subsurface (e.g., chromium-steel interface) barrel temperatures. To validate such models, it is necessary to fire live ammunition. Three 120 mm round types, viz., M865, M829, and DM13 were used for this purpose. The M865 is a US-made, cone-stabilised, discarding sabot, kinetic energy (KE) penetrator designed for target-practice. The M829 is a US-made, fin-stabilised, discarding sabot, KE service round, as is the German-made DM13. All three rounds use different propellant formulations, and this factor provides a range of heat input to the barrel.

The M865 and M829 cartridges were fired in a chromium-plated gun tube instrumented by personnel from the US Army Combat Systems Test Activity (CSTA), using Veritay Technology, Inc., in-wall thermocouple (IWTC) probes (Fig. 1). The probes were

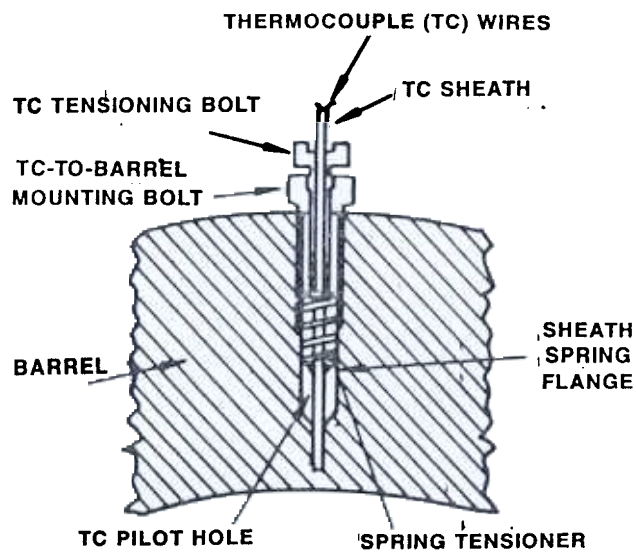

Figure 1. Typical veritay IWTC installation.

Received 13 November 1995, revised 08 April 1996

installed at each of three circumferential positions (starting at the top and spaced 120° apart) at each of four axial locations along the gun tube. The wall thickness was measured ultrasonically, and the IWTC holes were drilled to within 1.27 mm of the bore surface. A spring tensioner was used to hold the thermocouple (TC) junction against the bottom of the hole. Prior to firing, the M865 rounds were conditioned at 21 °C, and the M829 rounds were conditioned at 21 °C and 49 °C. Figure 2 displays a drawing of the instrumented gun tube.

A second gun tube was instrumented with welded thermocouples, and a preliminary DM13 round conditioned at about 21 °C was fired; this round served as a warmer round as well as a preliminary IWTC instrumentation checkout round. Due to unexpected data acquisition problems for this DM13 round, only one data channel was recorded, corresponding to an IWTC probe location at 457 mm from the rear face of the tube (RFT). Figure 3 displays a representation of the welded IWTC, which was attached to the barrel by arcing the constantan wire to the grounded barrel. Figure 4 displays a drawing of the instrumented gun tube. It is noted that the 457 mm (18 in) probe location for this DM13 round actually corresponds to the chamber surface, and not to the bore surface.

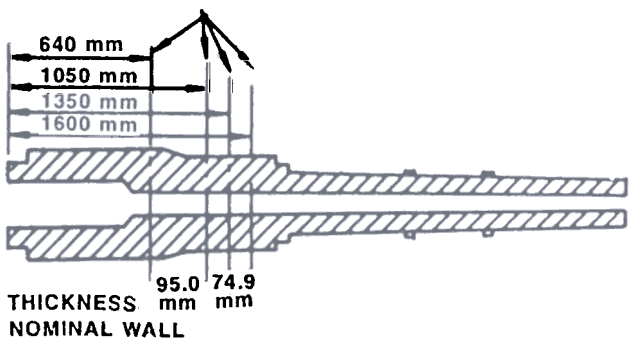

Figure 2. Modifications to M256 120 mm gun, serial no. 91

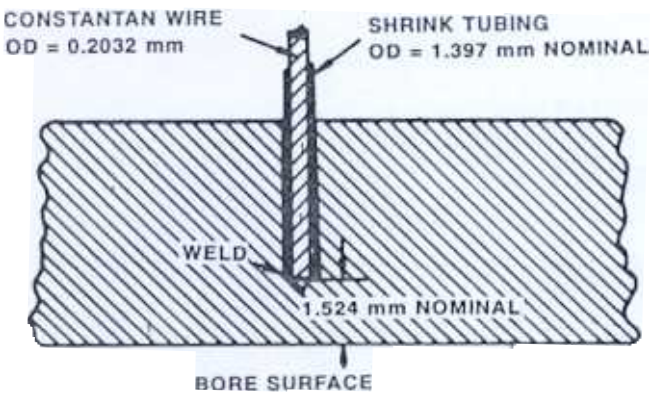

Figure 3. Typical welded IWTC installation.

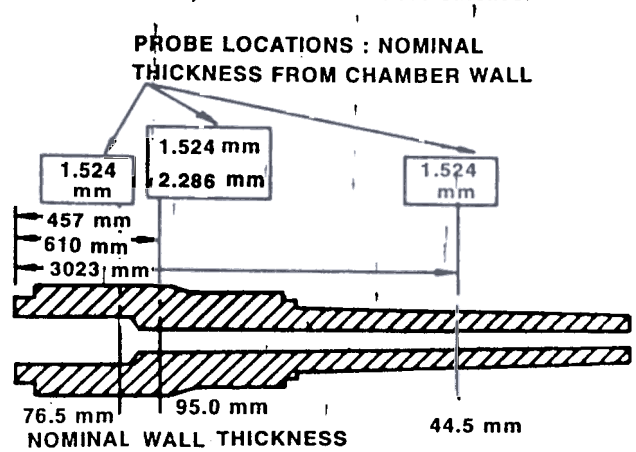

Figure 4. Modifications to M256 120 mm gun, serial no. 1910.

All simulations are derived from XKTC and XBR2D-V29 finite difference calculations[2,3]. (This version of XBR2D-V29 code is based on the program originated by Veritay Technology, Inc., and now incorporates revisions introduced by the US Army Research Laboratory (ARL). The thermal output of this calculation method has been successfully demonstrated in past simulation studies[4,5].

In this study, we chose the following thermal and mechanical properties for the barrel as input for the XBR2D-V29 code:

Chromium thickness: 0.14 mm

Chromium thermal conductivity: 84 J/(m-s-K)

Chromium thermal diffusivity: 2.3E-05 m^2/s

Steel thermal conductivity: 38 J/(m-s-K)

Steel thermal diffusivity: 1.0E-05 m^2/s

2. SIMULATED BORE SURFACE TEMPERATURES

Figures 5(a)-(d) display four plots of the simulated bore surface temperatures for M865 (21 °C), M829 (21 °C and 49 °C), and DM13 (21 °C) cartridges. The M865 and M829 plots show curves for four axial locations along the gun tube, whereas the DM13 plot displays only a single location, and this location corresponds to the chamber instead of the bore.

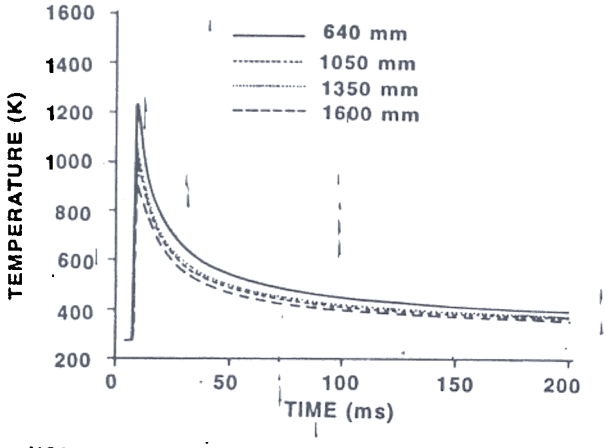

Figure 5a. Simulated bore surface temperatures for M865 (21 °C).

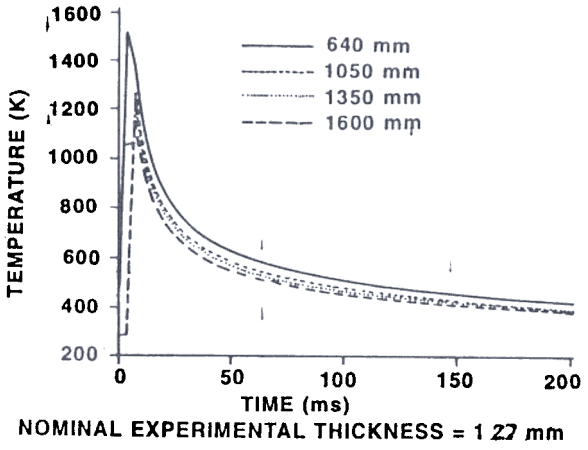

Figure 5c. Simulated bore surface temperatures for M829 (49 °C).

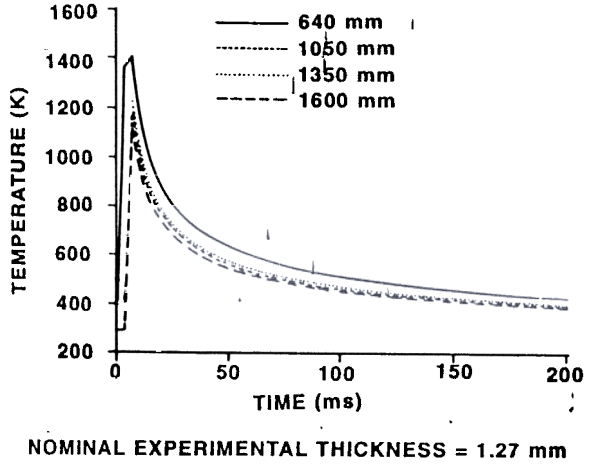

Figure 5b. Simulated bore surface temperatures for M829 (21 °C).

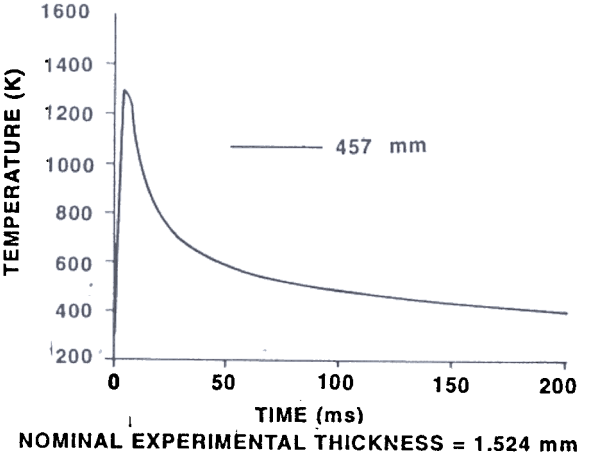

Figure 5d. Simulated chamber surface temperatures for DM13 (21 °C).

It is observed from these plots that the predicted bore surface temperatures generally decrease with increasing distance from the chamber. However, in the case of M865 and M829 rounds at 21 °C, the 1,350 mm curve is shown to be slightly higher than the 1,050 mm curve.

From Figure 5(b), the predicted peak bore surface temperatures, after firing an M829 at 21 °C, are about 1,405 K and 1,225 K at 640 mm and 1,350 mm from the RFT, respectively. A similar calculation was done by Bundy, Gerber, and Bradley for the same ammunition and initial conditions, but a different chromium thickness, using a different numerical treatment[6]. For a chromium thickness set at 0.10 mm, they predicted peak bore surface temperatures of about 1,650 K and 1,425 K at 700 mm and 1,400 mm from the RFT, respectively. With the chrome thickness set at 0.16 mm, they predicted about 1,200 K and 1,050 K, respectively. Thus, the predictions of Fig. 5, which are based on a chromium layer of 0.14 mm, are in close proximity to the Bundy, Gerber, and Bradley calculations[6]. This also shows how sensitive the peak surface temperature is to chrome thickness.

It was noted that in no case is the predicted bore surface temperature high enough to melt the chromium layer (having a melting temperature near 2,130 K). This is consistent with the fact that even though chromium can be found missing in M256 gun barrels, there has

never been any indication that it is missing due to melting; rather, it appears to spall-off.

The predicted bore surface temperature is the lowest for M865 at 21 °C and the highest for M829 at 49 °C and is confirmed to be true by experimental data (as is shown later).

3. EXPERIMENTAL IWTC PROBE TEMPERATURES

Figures 6(a)-(d) display individual plots of experimental probe measurements at 21 °C for each of two different cartridge types (M829 and DM13). In the case of M829 cartridge type, plots for three different test rounds are displayed, i.e., for round no. 2, round no. 6, and round no. 10, all at 640 mm from RFT (other round numbers corresponded to different ammunition).

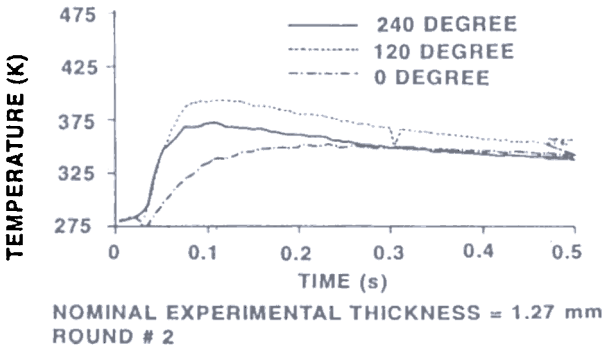

Figure 6a. M829 experimental probe temperatures at 21 °C for circumferential positions at 640 mm from RFT—round no. 2.

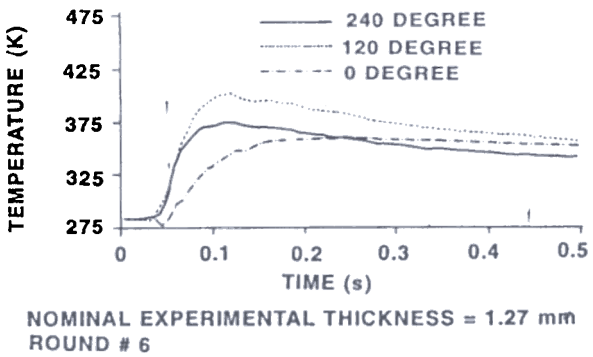

Figure 6b. M829 experimental probe temperatures at 21 °C for circumferential positions at 640 mm from RFT—round no. 6.

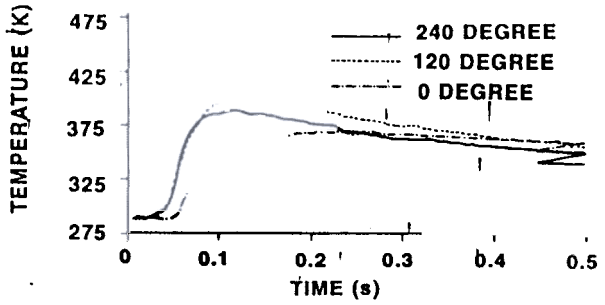

Figure 6c. M829 experimental probe temperatures at 21 °C for circumferential positions at 640 mm from RFT—round no. 10.

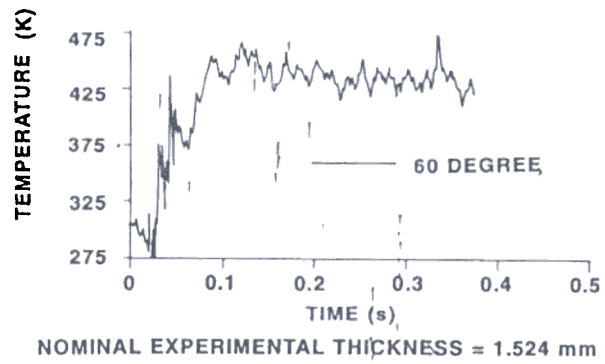

Figure 6d. DM13 experimental probe temperatures at 21 °C at 457 mm from RFT.

Each curve within each plot is designated by its round number together with its circumferential position in degrees. For example, No. 2/120 represents round no. 2, for the probe positioned at 120° from the top of the gun tube in the clockwise direction, looking from the breech to the muzzle.

From the data, it is obvious that the temperature at the three circumferential locations vary significantly and that the variations are estimated from the visual appraisal of their (pooled) mean profile to be as much as 25 per cent. In addition to the difference in magnitude, the initial rise rate of the 0° probe is distinctly different from the 120° and 240° probes. Furthermore, the ordering of the discrepancies in the circumferential probe temperatures is the same for all three M829 rounds (i.e., 120° > 240° > 0°) at this axial

location. Several reasons for such discrepancy may be speculated, and these include:

(a) Nonuniform thickness of metal (steel and chromium) between the bore surface and the probe tip.

(b) Variation in contact resistance between steel and chromium interfaces (e.g., partial chromium delamination).

(c) Nonuniform contact between IWTC probe tip and metal substrate (e.g., oil/dirt contamination).

(d) Nonuniform circumferential heat input.

Most likely, reason (a) is the largest contributor to the discrepancy in circumferential probe temperatures. In subsequent plots, it is shown that a variation in the metal thickness between the probe tip and the bore surface of from 0.25 to 0.50 mm would account for the circumferential temperature inconsistency. In this regard, an error is anticipated in the IWTC depth (due to an uncertainty in the barrel wall thickness at the location where each probe hole was drilled) of from 0.1 to 0.3 mm. The data further indicate that the probe temperatures at the same axial and circumferential location can vary by as much as 20 per cent from one round to the next.

Even though it is unlikely the cause of the circumferential temperature differences in Fig. 6, variation in contact resistance at the chromium-steel interface, reason (b) could be caused by localised delamination of chromium from steel. Figure 7 illustrates, from a different barrel, how the chromium layer can locally separate from the steel, leading to filling up of the voids by non-thermally conducting material, such as plastic from the obturator band.

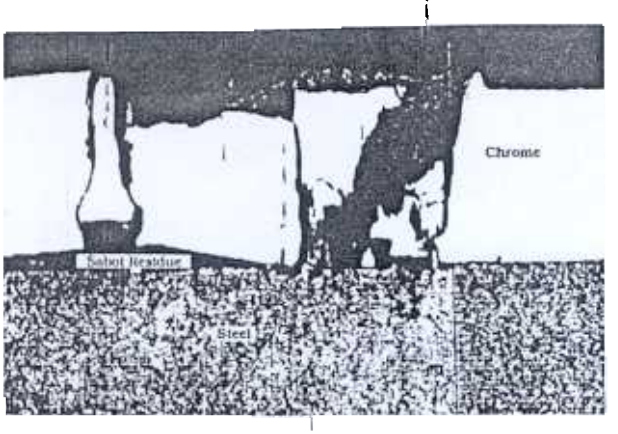

Figure 7. Photomicrograph of chrome-steel interface showing debonding voids filled by sabot material residue (courtesy: Joe Cox, Benet Laboratory).

A single plot for the DM13 round is included within Fig. 6 to compare with the M829 round. The plots are expected to differ from the standpoints of probe location and probe type (i.e., locations at 640 mm versus 457 mm, and Veritay versus welded IWTC probe types, respectively).

4. SIMULATED VERSUS EXPERIMENTAL IWTC PROBE TEMPERATURES

The authors are unable to display a complete set of circumferential probe measurements at each axial location, nor give, with confidence, the circumferentially averaged probe temperature at each axial location, due to improper functioning of one or more IWTC probes at each axial location, except 640 mm. Nevertheless, at least one experimental probe temperature at every axial location in the comparison of theory with experiment, is presented here.

Simulated temperature estimates with IWTC probe for four different rounds (DM13, M865, and M829 at 21 °C and 49 °C) along with measured temperatures are presented in Figs 8, 9, 10, and 11.

For all plots, simulated curves, differing by depth increments of 0.254 mm, are superimposed over each experimental curve for the specified axial location. Thus, the experimental curve, with assumed probe depth, say, of 1.27 mm, is bracketed by simulated curves of lesser and/or greater presumed depths. In addition, the initial barrel temperature has been simulated to match the initial measured barrel temperature at the circumferential and axial location of the round identified in the experimental curve on each plot, in every figure.

4.1 DM13 Round (21 °C)

Figure 8 displays simulated curves corresponding to probe depths of 1.016, 1.27, and 1.52 mm. Also superimposed on this plot is the experimental curve corresponding to an assumed depth of 1.524 mm. Noise in this experimental curve is believed to be due to the large distance between the IWTC probe and the amplifier. The other probable reasons could be induced currents caused by ground loop from wet lines and line whipping during gun recoil. Underlying the noise, the experimental curve matches the rise rate and magnitude of the 1.27 mm simulated depth curve better than the 1.52 mm simulation.

It should be noted that, in this comparison, the IWTC probe is located in the chamber region of the

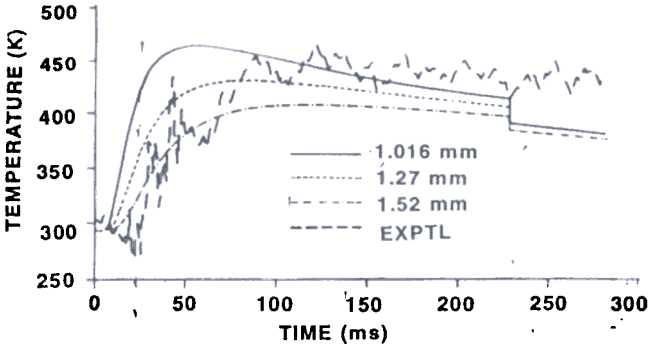

Figure 8. DM13 simulated and experimental probe temperatures at 21 °C.

barrel, where, presumably, the combustible cartridge case partially insulates the surface from direct exposure to the propellant gases until the case has been consumed. The effect of the randomly breaking/burning cartridge case has not been incorporated into XBR2D-V29, as yet. Thus, it is not surprising that theory and experiment are not in agreement in the chamber region, even if the probe depth is, indeed, 1.52 mm.

4.2 M865 Round (21 °C)

Figures 9(a)-(d) display four plots for the M865 round, conditioned to 21 °C at axial probe locations of 640, 1,050, 1,350, and 1,600 mm. The simulated curves represent depths of 1.27, 1.52, and 1.78 mm with the exception of Fig. (9b), where an additional depth of 1.016 mm is also displayed. It is apparent that these curves generally bracket the superimposed

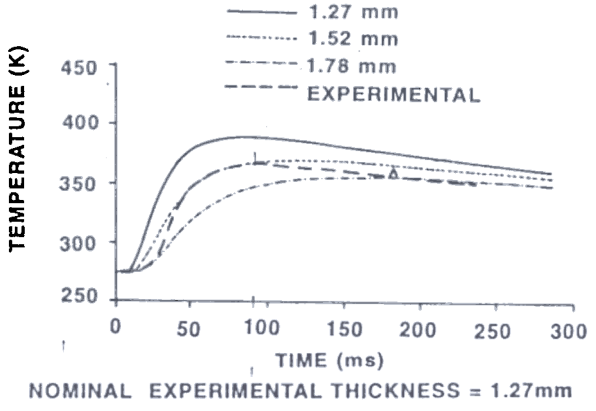

Figure 9a. M865 simulated and experimental probe temperatures at 640 mm from RFT at 21 °C—round no. W2/240.

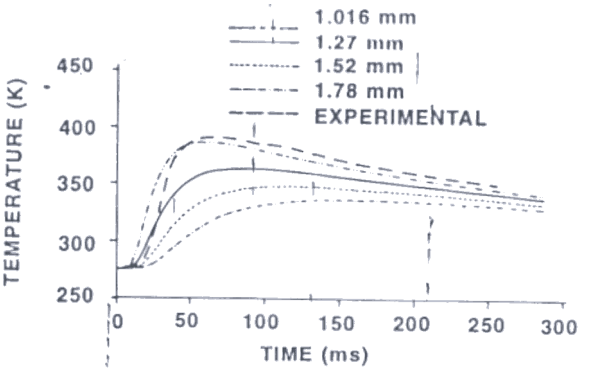

Figure 9b. M865 simulated and experimental probe temperatures at 1050 mm from RFT at 21 °C—round no. W2/120.

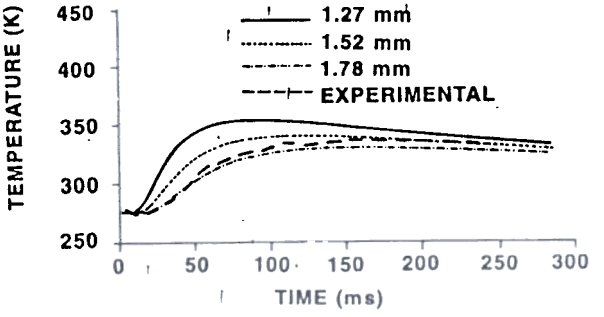

Figure 9c. M865 simulated and experimental probe temperatures at 1350 mm from RFT at 21 °C—round no. W2/0.

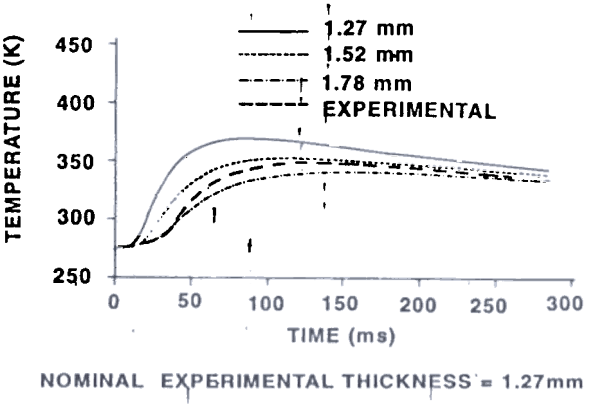

Figure 9d. M865 simulated and experimental probe temperatures at 1600 mm from RFT at 21 °C—round no. W2/0.

experimental curve at an assumed depth of 1.27 mm. The differences in shape and magnitude of the simulated temperature versus time plots from a probe depth of 1.27 mm to a probe depth of 1.78 mm are nearly identical to the range of shape and magnitude differences shown in Figs 6(a)-(c). This supports the conjecture that circumferential temperature discrepancies are most likely due to circumferential variation in the probe depths.

4.3 M829 Round (21 °C)

Figures 10(a)-(d) display four plots for the M829 round, conditioned at 21 °C, at axial probe locations of 640, 1,050, 1,350, and 1,600 mm. It is noteworthy that horizontal (time) translation of all simulated curves by approximately 40 ms would yield better agreement

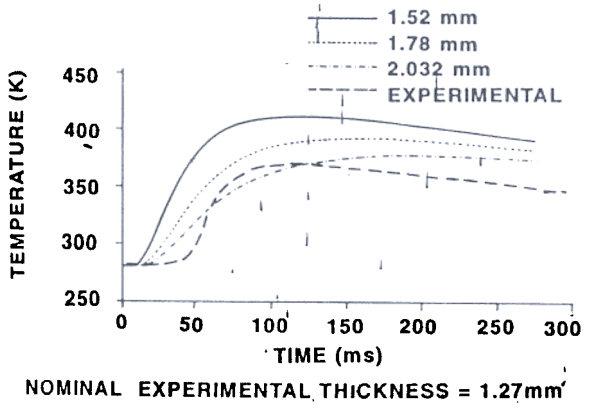

Figure 10a. M829 simulated and experimental probe temperatures at 640 mm from RFT at 21 °C—round no. 6/240.

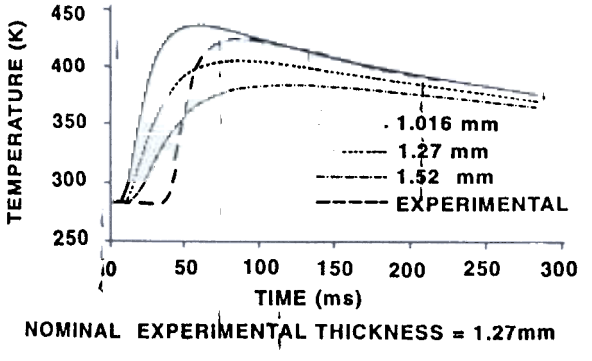

Figure 10b. M829 simulated and experimental probe temperatures at 1050 mm from RFT at 21 °C—round no. 6/120.

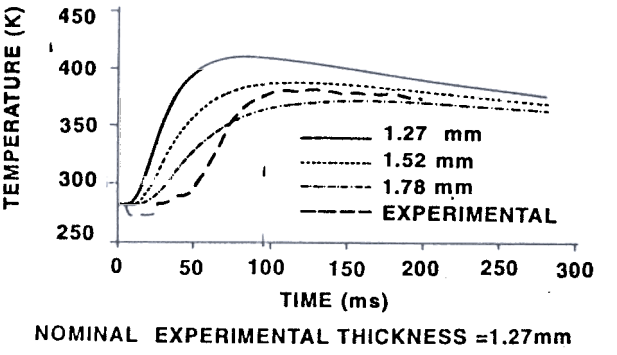

Figure 10c. M829 simulated and experimental probe temperatures at 1350 mm from RFT at 21 °C—round no. 6/0.

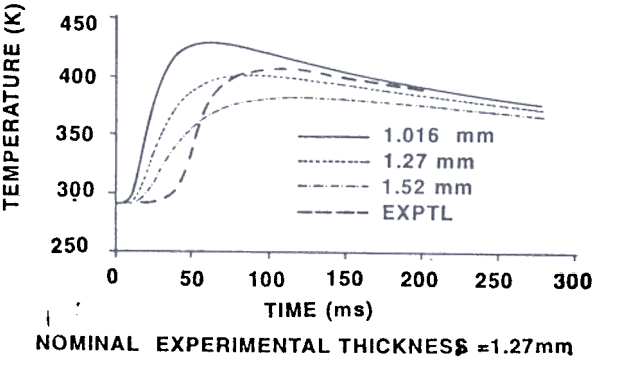

Figure 10d. M829 simulated and experimental probe temperatures at 1600 mm from RFT at 21 °C—round no. 10/240.

between experimental and simulated curves in most cases. Though some of this temporal disparity may be due to an overly simplistic model of the ignition delay and flame spreading process, it is believed that the majority of time difference is due to uncertainty in the experimental ignition fiduciary.

It can be seen from Figs 9 and 10 that the M829 round produces a greater barrel temperature rise than the M865 round at all axial locations. This experimental result is consistent with the ordering of the simulated bore surface temperatures in Fig. 5.

4.4 M829 Round (49 °C)

Figures 11(a)-(d) are a set of plots which are counterparts to Figs 10(a)-(d) (i.e., same type of round) but at higher conditioning temperature. The behaviour

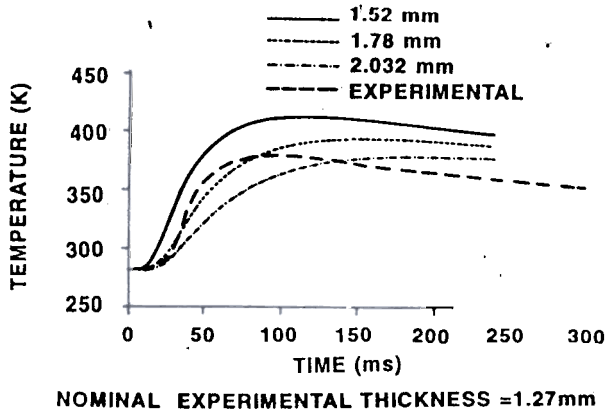

Figure 11a. M829 simulated and experimental probe temperatures at 640 mm from RFT at 49 °C—round no. 4/240.

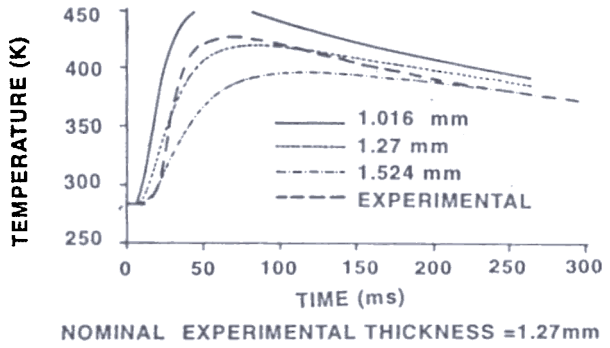

Figure 11b. M829 simulated and experimental probe temperatures at 1050 mm from RFT at 49 °C—round no. 4/120.

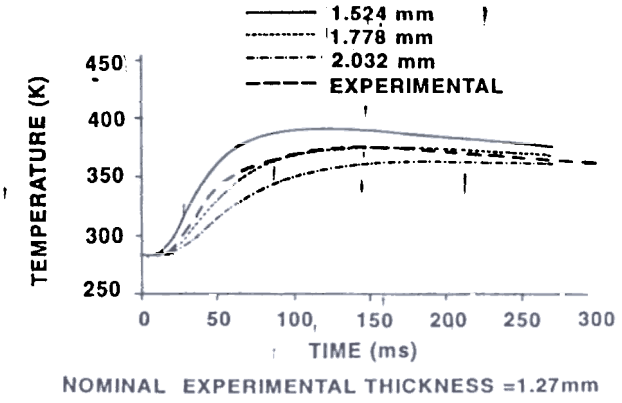

Figure 11c. M829 simulated and experimental probe temperatures at 1350 mm from RFT at 49 °C—round no. 4/240.

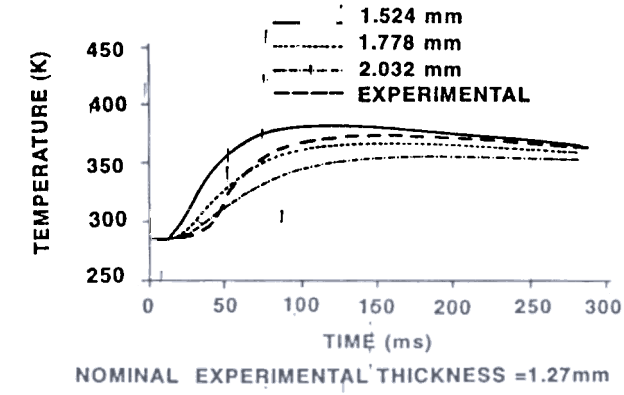

Figure 11d. M829 simulated and experimental probe temperatures at 1600 mm from RFT at 49 °C—round no. 4/0.

is similar at both the conditioning temperatures except that the required temporal translation of the time axis is not as great for the 49 °C plots as for the 21 °C plots. Even though the simulated bore surface temperatures are higher for the higher preconditioned round temperature, a noticeable difference was not detected in the IWTC measurements between an M829 at 21 °C and an M829 at 49 °C. It is suspected that the effect of preconditioning is masked by the inherent round-to-round variation (Fig. 6) in barrel heat input and the small sample size tested.

Overall, the experimental temperature histories, in conjunction with the simulations in Figs 9-11, corroborate each other, wherever two or more plots reference the same probe, with regard to indicating the probable IWTC depth. The examples are as follows:

Figures 9(c) and 10(c) indicate the probe depth at 1,350 mm and 0° (top) from RFT is between 1.52 and 1.78 mm below the bore surface. Furthermore, Figs 9(d) and 11(d) point to the same depth for the probe 1,600 mm and 0° from RFT. Figures 9(a), 10(a), and 11(a) all reference the IWTC at 640 mm and 240° from RFT. In all cases, the temperature rise rate of the experimental curve matches with the of the simulated curve for a probe depth of between 1.27 and 1.52 mm. However, the magnitude of the experimental curve is between the simulated curve depths of 1.52 and 2.03 mm. Unlike the other axial locations, the probe at 640 mm is in the saddle region of the sabot, which means the front bore rider on the sabot does not cross under the IWTC. Does this make a difference or is the flow pattern just downstream from the chambrage different

than currently modelled? These questions are not answered here. Lastly, Figs 9-11 consistently show that the probe temperature at 1,050 mm and 120° is higher than in any other location. But, rather than conclude that the firing heat input is simply higher at this location, Figs 9(b), 10(b), and 11(b) all suggest that it is higher than elsewhere because the probe is closer here than elsewhere probably lying between 1.02 mm and 1.27 mm below the surface.

5. SUMMARY

The XBR2D-V29 heat transfer/conduction code. as revised by ARL, has been used in conjunction with the XKTC interior ballistic code to provide barrel temperature predictions for the M256 120 mm cannon firing various ammunition. It is found that the predicted bore surface temperature is consistent with that reported elsewhere. The experimental barrel temperature data taken from IWTC near the barrel's inner wall is also shown. The predictions agree reasonably well with the experimental results. For the most part, discrepancies in the temperature profile between experimental and simulated curves are compatible with the presumed error in the probe depth, and round-to-round variation. Nevertheless, the areas where helpful modifications might be made would include: (i) a modelling option for combustible cartridge case effects in the XBR2D-V29 code, (ii) a refinement of the timing involved in the ignition delay and flame spreading process in the XKTC code, and (iii) a reassessment of the downbore flow field model near the chambrage.

ACKNOWLEDGMENT

The authors wish to acknowledge Mr Harold R. Bowers, U.S. Army Aberdeen Test Center, for his assistance involving in-wall thermocouple probe installation and data acquisition.

REFERENCES

1. Brosseau, T. L. An experimental method for accurately determining the temperature distribution and the heat transferred in gun barrels. US Army Ballistic Research Laboratory, Aberdeen Proving Ground, MD, September 1974. BRL-R-1740.
2. Gough, P. S. The XNOVAKTC code. US Army Ballistic Research Laboratory, Aberdeen Proving Ground, MD, February 1990. BRL-CR- 627.
3. Crickenbeger, A.B.; Talley, R.L. & Talley, J.Q. Modifications to the XBR2D heat conduction code. US Army Research Laboratory, Aberdeen Proving Ground, MD, April 1994. ARL-CR- 126.
4. Conroy, P.J. Gun tube heating. US Army Ballistic Research Laboratory, Aberdeen Proving Ground, MD, December 1991. BRL- TR-3300.
5. Keller, G.E.; Horst, A.W.; Conroy, P.J. & Coffee, T.P. The influence of propulsion technique and firing rate on thermal management problems in large-calibre guns. US Army Research Laboratory, Aberdeen Proving Ground, MD, May 1993. ARL-TR- 130.
6. Bundy, M.; Gerber, N. & Bradley, J.W. Evaluating potential bore melting from firing M829A1 ammunition. US Army Research Laboratory, Aberdeen Proving Ground, MD, October 1993. ARL-MR-107.

Contributors

Dr Mark Bundy obtained his PhD in Physics in 1980 from the University of Maine, Orono, ME in 1980. He is currently working on the problem of evaluating heat transfer modes for gun barrels at the US Army Research Laboratory, Aberdeen Proving Ground, MD. He has considerable experience in the thermal management for the improvement of tank gun accuracy.

Mr Paul Conroy completed his MS (Mechanical Engineering) from the Pennsylvania State University, US, in 1989. He is working as Mechanical Engineer at the US Army Research Laboratory, Aberdeen Proving Ground, MD. He has worked on cryogenics at the Fermi National Accelerator Laboratory, Batavia, IL.

Mr James Kennedy obtained his MS in Mechanical Engineering from the National Technological University. Presently, he is working as Principal design engineer at the Alliant Techsystems (ATK), Hopkins, MN. Earlier, he provided tank ammunition propulsion support at Honeywell/ATK for 15 years. At present, he holds four patents.